Modern Physics Letters A

IMPLEMENTATION OF THE ATLAS-SUSY-2018-17 ANALYSIS IN THE MADANALYSIS 5 FRAMEWORK

TAYLOR MURPHY

Department of Physics, The Ohio State University
191 W. Woodruff Ave., Columbus, OH 43210, U.S.A.
murphy.1573@osu.edu

We present the implementation in MadAnalysis 5 of ATLAS-SUSY-2018-17, a search for new phenomena in final states with large jet multiplicities and missing transverse momentum, and detail the validation of this implementation. This ATLAS analysis targets new particles decaying into eight or more jets and significant missing transverse energy ($E_{\mathrm{T}}^{\mathrm{miss}}$) using $\mathcal{L} = 139\,\mathrm{fb}^{-1}$ of proton-proton (pp) collisions at the LHC at a center-of-mass energy of $\sqrt{s} = 13\,\mathrm{TeV}$. We validate our implementation by simulating gluino pair production in a simplified model with gluinos decaying in cascades to quarks, weak bosons, and (lightest) neutralinos — for example,

$$pp \to \tilde{g}\tilde{g}, \quad \tilde{g} \to u\bar{d} + \tilde{\chi}_1^- \ \textit{via}\ \text{off-shell}\ \tilde{u}_{\mathrm{L}}, \quad \tilde{\chi}_1^- \to W^-\tilde{\chi}_2^0, \quad \tilde{\chi}_2^0 \to Z\tilde{\chi}_1^0$$

— and comparing event yields after selection cuts to those provided by ATLAS at a particular point in this model's parameter space. We find acceptable agreement with the official cut-flows and consider this implementation validated.

Keywords: Multijet events, supersymmetric models, cascade decays

1. Introduction

The second run of the Large Hadron Collider (LHC) has produced an integrated luminosity of $\mathcal{L} \approx 140\,\mathrm{fb}^{-1}$ of proton-proton (pp) collisions at a center-of-mass energy of $\sqrt{s} = 13\,\mathrm{TeV}$. The excellent performance of the LHC, alongside increasingly sophisticated analysis by the ATLAS and CMS collaborations, offers an unprecedented opportunity to explore physics beyond the Standard Model (bSM) — particularly complex scenarios with high jet multiplicities and significant amounts of missing transverse energy ($E_{\mathrm{T}}^{\mathrm{miss}}$). Supersymmetry (SUSY), which remains a leading candidate for bSM physics, can be realized in a panoply of models featuring cascade decays of heavy new species to SM particles alongside invisible light (and possibly stable) new particles. Some such models are expected to produce signatures at the LHC consisting not only of large numbers of jets but also of large-radius jets with masses greater than that of the top quark ($m_t \approx 175\,\mathrm{GeV}$), in stark contrast to SM multijet signatures.

The ATLAS collaboration has published a search for new phenomena producing

signatures of this class in a report initially designated as ATLAS-CONF-2020-002[a] and published with updates and additional material as ATLAS-SUSY-2018-17.[2] This search requires at least eight jets and imposes additional requirements on b-tagged jets and large-radius jets while vetoing isolated electrons and muons. ATLAS reports no evidence for physics beyond the Standard Model from this search, and interprets results in the context of three simplified models of gluino pair production, $pp \to \tilde{g}\tilde{g}$, with each gluino decaying to some set of SM particles in addition to an invisible particle inspired by the lightest neutralino $\tilde{\chi}_1^0$ in models where it is the lightest supersymmetric particle (LSP). ATLAS is able to extend lower limits on the gluino mass $m_{\tilde{g}}$ in these models to 1.5–2.0 TeV, with improvements in all cases of several hundred GeV over similar previous analyses.[3–7]

As we alluded to above, there are many models featuring pair production of heavy (s)particles with subsequent cascade decays to both light- and heavy-flavor quarks and missing energy. In particular, models of new physics that enhance the LHC production of four top quarks ($t\bar{t}t\bar{t}$) are quite common. One well motivated example is the family of models with "supersoft" D-term SUSY breaking and (pseudo-)Dirac gauginos, which predict copious pair production of color-octet scalars (*sgluons*) decaying with varying branching fractions to $t\bar{t}$.[8] In these models, there are regions of parameter space where the sgluon-mediated production of four top quarks is kinematically distinct from SM four-top production and is well suited to be probed by multijet + $E_{\mathrm{T}}^{\mathrm{miss}}$ searches like ATLAS-SUSY-2018-17.[9] This is just one example of how it is in the community's interest to be able to interpret this analysis in models not considered by ATLAS. The MadAnalysis 5 framework, which provides a platform to emulate each step of an LHC analysis from detector simulation and object reconstruction to event selection, makes this goal achievable.[10–12] In this note, we describe how we have implemented the ATLAS-SUSY-2018-17 analysis in this framework in order to apply it to arbitrary models of new physics. This note is a minor update of the validation note for ATLAS-CONF-2020-002. It shares a great deal of text with that note but includes an improved validation made possible by ATLAS' inclusion of cut-flows in the updated analysis.

This note is organized as follows. In Section 2, we reproduce the salient details of the ATLAS-SUSY-2018-17 analysis, including object definitions and event selection, and we explain how we have emulated this analysis in the MadAnalysis 5 framework. We present the validation of our implementation in Section 3, describing the simulation of events in a simplified model of gluino pair production and cascade decay, and providing cut-flows for comparison to those published by the ATLAS collaboration. We demonstrate acceptable agreement between our results and the official yields. We summarize this note in Section 4.

[a]This earlier version of the analysis has already been implemented in MadAnalysis 5.[1]

Criterion	Electrons	Muons	Photons	Jets	b-tagged jets
p_{T} [GeV]	> 7.0	> 6.0	> 40	> 20 $[R = 0.4]$ > 100 $[R = 1.0]$	> 20
$\lvert\eta\rvert$	< 2.47	< 2.7	< 2.37 and $\notin (1.37, 1.52)$	< 2.8 $[R = 0.4]$ < 1.5 $[R = 1.0]$	< 2.5

Table 1: Summary of preselection criteria, reproduced in part from Section 4 of ATLAS-SUSY-2018-17.[13]

2. Description of the analysis

ATLAS-SUSY-2018-17 looks for new phenomena in final states with large numbers of jets and significant missing transverse energy. It particularly targets events with at least eight anti-k_t radius $R = 0.4$ jets with transverse momentum $p_{\mathrm{T}} > 50\,\mathrm{GeV}$ or higher, depending on signal region. It also requires a high missing transverse energy significance $\mathcal{S}(E_{\mathrm{T}}^{\mathrm{miss}})$ in order to disambiguate genuine $E_{\mathrm{T}}^{\mathrm{miss}}$ associated with non-interacting particles from specious missing energy due to mismeasurements and fluctuations. This search vetoes virtually all leptons surviving an overlap-removal procedure. The final noteworthy element of this search is a set of cuts on the cumulative mass M_{J}^{Σ} of high-p_{T} large-radius (anti-k_t radius $R = 1.0$) jets, which is intended to stringently control the SM multijet background. Here we discuss these criteria in some more detail and offer notes about our implementation of this analysis in MadAnalysis 5.

2.1. *Object definitions*

ATLAS-SUSY-2018-17 comprises a multi-bin and a single-bin subanalysis, the latter of which defines eight non-overlapping signal regions. We have implemented the single-bin subanalysis in MadAnalysis 5. The signal object candidates are required to satisfy several kinematic criteria and to pass a multi-step procedure for overlap removal. The most important preselection criteria are summarized in Table 1, but we comment more on particle reconstruction here.

Jets are reconstructed using the anti-k_t algorithm[14] and are clustered twice. The primary collection of jets has anti-k_t radius parameter $R = 0.4$. These jets must have transverse momentum $p_{\mathrm{T}} > 20\,\mathrm{GeV}$ and pseudorapidity $|\eta| < 2.8$, except for the calculation of missing transverse energy, $E_{\mathrm{T}}^{\mathrm{miss}}$, for which the latter constraint is relaxed to $|\eta| < 4.5$. There is a second collection of large-radius ("fat") jets with radius parameter $R = 1.0$, $p_{\mathrm{T}} > 100\,\mathrm{GeV}$, and $|\eta| < 1.5$. Narrow $R = 0.4$ jets with $|\eta| < 2.5$ containing b-hadrons are identified as b-tagged jets if the discriminant output of a multivariate algorithm[15] exceeds a threshold resulting in an average b-jet identification efficiency of 70% for jets containing b-hadrons in simulated $t\bar{t}$ events.[16]

Leptons are subject to relatively mild kinematic requirements. Baseline electrons must have $p_{\mathrm{T}} > 7\,\mathrm{GeV}$ and $|\eta| < 2.47$, and baseline muons must satisfy $p_{\mathrm{T}} > 6\,\mathrm{GeV}$

and $|\eta| < 2.7$. The minimum transverse momentum requirements are raised to $p_{\mathrm{T}} > 20\,\mathrm{GeV}$ for signal electrons and signal muons. These objects are primarily used in leptonic control regions, with all baseline leptons with $p_{\mathrm{T}} > 10\,\mathrm{GeV}$ ultimately vetoed in all eight signal regions.

Photons are required to satisfy $p_{\mathrm{T}} > 40\,\mathrm{GeV}$ and $|\eta| < 2.37$. An additional pseudorapidity "crack" veto, $|\eta| \notin (1.37, 1.52)$, is applied to avoid a region of the calorimeter with limited instrumentation.

An overlap-removal procedure is applied to the baseline objects described above in order to resolve reconstruction ambiguities. First, any electron sharing an inner detector track with a muon is rejected. Next, photons with angular distance $\Delta R < 0.4$ from any lepton are discarded. ATLAS uses a standard definition of angular distance,

$$\Delta R = \sqrt{(\Delta y)^2 + (\Delta\phi)^2} \quad \text{with} \quad y = \frac{1}{2}\ln\frac{E + p_z}{E - p_z},$$

in which the rapidity y is defined in terms of the energy E and component p_z of momentum along the beam direction, and ϕ is the azimuthal angle about the beam (z) axis. Following the photon removal, non-b-tagged jets are rejected if closer than $R = 0.2$ to an electron. Finally, leptons within $\Delta R = 0.4$ of a surviving jet are removed, and then jets closer than $\Delta R = 0.4$ to any photon are eliminated. We have implemented all the criteria explicitly mentioned here in the MadAnalysis 5 framework, but it should be noted that there are some additional overlap removal criteria, including *e.g.* restrictions on the number of jet tracks and electron p_{T} ordering, that are not implemented.

The missing transverse energy, $E_{\mathrm{T}}^{\mathrm{miss}}$, is defined as the magnitude of the negative vector sum of the transverse momenta of all signal candidates that pass the overlap removal procedure:

$$E_{\mathrm{T}}^{\mathrm{miss}} = \left| -\sum_i \left[\vec{p}_{\mathrm{T}i}^{\,\mathrm{jet}} + \vec{p}_{\mathrm{T}i}^{\,\mathrm{electron}} + \vec{p}_{\mathrm{T}i}^{\,\mathrm{muon}} + \vec{p}_{\mathrm{T}i}^{\,\mathrm{photon}} \right] \right|.$$

Whereas often a selection cut is imposed on the magnitude of $E_{\mathrm{T}}^{\mathrm{miss}}$, ATLAS-SUSY-2018-17 requires a minimum missing transverse energy significance $\mathcal{S}(E_{\mathrm{T}}^{\mathrm{miss}})$. This object is designed to distinguish transverse momentum carried by non-interacting particles from $E_{\mathrm{T}}^{\mathrm{miss}}$ that should be attributed elsewhere. ATLAS has begun to use an "object-based" definition of $\mathcal{S}(E_{\mathrm{T}}^{\mathrm{miss}})$, based on the kinematic qualities and resolutions of each object in an event, given by[17]

$$\mathcal{S}(E_{\mathrm{T}}^{\mathrm{miss}}) = \frac{E_{\mathrm{T}}^{\mathrm{miss}}}{\sqrt{\sigma_{\mathrm{L}}^2(1 - \rho_{\mathrm{LT}}^2)}},$$

where σ_{L} is the total expected longitudinal resolution of all objects in the event as a function of the p_{T} of each object, and ρ_{LT} is the correlation factor between all longitudinal and transverse object resolutions. This definition of $\mathcal{S}(E_{\mathrm{T}}^{\mathrm{miss}})$ outputs a pure number, which ATLAS-SUSY-2018-17 requires to exceed 5.0. Unfortunately, this measure of $\mathcal{S}(E_{\mathrm{T}}^{\mathrm{miss}})$ cannot be implemented in MadAnalysis 5 at this time. In

Selection criterion	Selection ranges
Jet multiplicity, N_{jet}	$N_{\text{jet}}^{50} \geq \{8, 9, 10, 11, 12\}$ $N_{\text{jet}}^{80} \geq 9$
Trigger thresholds	6 or 7 jets, $E_{\text{T}} > 45\,\text{GeV}$ 5 jets, $E_{\text{T}} > 65$ or $70\,\text{GeV}$
Lepton veto	0 baseline leptons, $p_{\text{T}} > 10\,\text{GeV}$
$E_{\text{T}}^{\text{miss}}$ significance, $\mathcal{S}(E_{\text{T}}^{\text{miss}})$	$\mathcal{S}(E_{\text{T}}^{\text{miss}}) > 5.0$

Table 2: Summary of common selection criteria, reproduced in part from Sections 4 and 5 and Table 1 of ATLAS-SUSY-2018-17.[13] Variable trigger thresholds depend on year in which data were collected.

keeping with other validated implemented searches available on the MadAnalysis 5 Public Analysis Database (PAD)[18] that have confronted this same problem, we have used a $\mathcal{S}(E_{\text{T}}^{\text{miss}})$ proxy,

$$\mathcal{S}_{\text{proxy}}(E_{\text{T}}^{\text{miss}}) = \frac{E_{\text{T}}^{\text{miss}}}{\sqrt{H_{\text{T}}}} \quad \text{with} \quad H_{\text{T}} = \sum_i p_{\text{T}i}^{\text{jet}}, \tag{1}$$

which was used by ATLAS prior to the adoption of the new object-based definition.[19] This proxy has units of $\text{GeV}^{1/2}$, so our cut is at $\mathcal{S}_{\text{proxy}}(E_{\text{T}}^{\text{miss}}) = 5\,\text{GeV}^{1/2}$.

2.2. *Event selection*

Selection cuts significantly more stringent than the preselection criteria are applied in the eight non-overlapping signal regions of ATLAS-SUSY-2018-17. All selection cuts other than those on jet multiplicity and cumulative fat-jet mass are applied to all signal regions. The common cuts are summarized in Table 2. All events featuring baseline leptons surviving the overlap-removal procedure with $p_{\text{T}} > 10\,\text{GeV}$ are rejected to control background from the SM processes $W \to \nu_\ell \ell$, which produce copious $E_{\text{T}}^{\text{miss}}$. Biases in $E_{\text{T}}^{\text{miss}}$ due to pile-up effects are accounted for by removing events containing jets azimuthally separated from $E_{\text{T}}^{\text{miss}}$ by $|\Delta\phi(\text{jet}, E_{\text{T}}^{\text{miss}})| > 2.2$. Standard baseline jets are promoted to signal jets if they have $p_{\text{T}} > 50\,\text{GeV}$ or $> 80\,\text{GeV}$, depending on signal region. All signal jets must have $|\eta| < 2.0$. The final common criterion is the minimum missing transverse energy significance: $\mathcal{S}(E_{\text{T}}^{\text{miss}}) > 5.0$ ($5.0\,\text{GeV}^{1/2}$ if using $\mathcal{S}_{\text{proxy}}(E_{\text{T}}^{\text{miss}})$; see Section 2.1 above).

Once the common criteria are applied, ATLAS-SUSY-2018-17 finally imposes unique restrictions on jets to define each signal region in the single-bin analysis. These signal region criteria are summarized in Table 3. The signal regions labeled by `SR-`N_{jet}^{50}`ij50-...` require the presence of at least N_{jet}^{50} jets with $p_{\text{T}} > 50\,\text{GeV}$, where $N_{\text{jet}}^{50} \in [8, 12]$. The first five of these signal regions further require the cumulative mass of the fat jets,

$$M_{\text{J}}^{\Sigma} = \sum_j m_j^{R=1.0},$$

Signal region	N_{jet}^{50}	N_{jet}^{80}	$N_{b\text{-jet}}$	M_{J}^{Σ} [GeV]
SR-8ij50-0ib-MJ500	≥ 8	-	-	≥ 500
SR-9ij50-0ib-MJ340	≥ 9	-	-	≥ 340
SR-10ij50-0ib-MJ340	≥ 10	-	-	≥ 340
SR-10ij50-0ib-MJ500	≥ 10	-	-	≥ 500
SR-10ij50-1ib-MJ500	≥ 10	-	≥ 1	≥ 500
SR-11ij50	≥ 11	-	-	-
SR-12ij50-2ib	≥ 12	-	≥ 2	-
SR-9ij80	-	≥ 9	-	-

Table 3: Summary of signal region criteria for single-bin selections, which appears in Table 3 of ATLAS-SUSY-2018-17.[13] A dash (-) indicates that no requirement is applied to the corresponding variable. The requirement $\mathcal{S}(E_{\text{T}}^{\text{miss}}) > 5.0$ is applied to all bins.

to equal or exceed 340 GeV or 500 GeV depending on signal region. Two of these signal regions finally require nonzero numbers of b-tagged jets. The signal region SR-9ij80 instead requires at least nine signal jets with $p_{\text{T}} > 80$ GeV. We note here that the common $E_{\text{T}}^{\text{miss}}$ significance cut is imposed after the specific jet multiplicity and mass cuts in each signal region.

We have written code in C++ that can be run in the reconstruction (-R) mode of MadAnalysis 5 to emulate the analysis described above and allow us to apply it to new event samples. Either for the purpose of validation, which is discussed in Section 3, or in order to analyze different models, we provide as input to MadAnalysis 5 some sample of hard-scattering events that have been matched to parton showers and hadronized. These showered and hadronized events are first passed by MadAnalysis 5 to Delphes 3 version 3.4.2[20] and FastJet version 3.3.3,[21] which respectively model the response of the ATLAS detector and perform object reconstruction. For this implementation, we use a Delphes 3 card for the ATLAS detector, a basic version of which is shipped with MadAnalysis 5, modified to include a collection of jets for both anti-k_t radius parameters ($R = 0.4$ and $R = 1.0$) required for this search. The b-jet tagging algorithm in this default card is tailored to match the performance of the multivariate algorithm used by ATLAS at the aforementioned 70%-efficiency operating point.[16] The reconstructed events are then analyzed by our reimplementation code, after which MadAnalysis 5 computes the acceptance of the event sample by the emulated selection criteria. With the acceptance(s) in hand, MadAnalysis 5 can use the CLs prescription[22] to compute the expected and observed upper limits at 95% confidence level (CL)

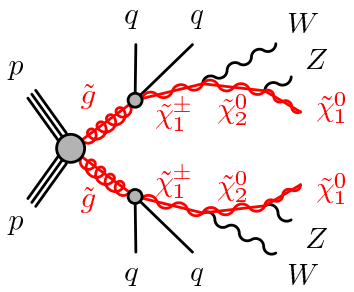

FIG. 1: Schematic diagram for the signal process $pp \to \tilde{g}\tilde{g}$, $\tilde{g} \to q\bar{q}' + WZ + \tilde{\chi}_1^0$, which appears in Figure 1(a) of ATLAS-SUSY-2018-17.[13] We simulate this process for $m_{\tilde{g}} = 1.60\,\text{TeV}$, $m_{\tilde{\chi}_1^0} = 100\,\text{GeV}$, and compare event yields after selection cuts to those provided by ATLAS in order to validate our implementation of the analysis.

on the number of signal events given the official numbers of expected background events and observed events. It can also extrapolate these limits to higher integrated luminosities, assuming no excess is found, with multiple approaches to background error propagation available to the user.[12]

3. Validation

While ATLAS-CONF-2020-002, the predecessor of ATLAS-SUSY-2018-17, does not provide detailed event yields for each selection cut in any signal region of the single-bin subanalysis, the updated analysis provides a set of cut-flows for one benchmark point in a particular simplified model inspired by common supersymmetric scenarios. In particular, ATLAS considers a model of gluino pair production, $pp \to \tilde{g}\tilde{g}$, in which each gluino undergoes a three-step[b] cascade decay consisting of the following steps:

$$\begin{aligned} pp \to \tilde{g}\tilde{g} \text{ followed by } \tilde{g} &\to q\bar{q}' + \tilde{\chi}_1^\pm \text{ (a three-body decay } \textit{via} \text{ virtual } \tilde{q}), \\ \tilde{\chi}_1^\pm &\to W^\pm \tilde{\chi}_2^0, \\ \text{and} \quad \tilde{\chi}_2^0 &\to Z\tilde{\chi}_1^0. \end{aligned}$$

The quarks must be light, $q, q' \in \{u, d, s, c\}$, and the final neutralino $\tilde{\chi}_1^0$ is assumed to be stable at least on collider timescales. The full cascade decay is assigned unit branching fraction. A diagram provided by ATLAS representing this process is reproduced in Figure 1. The independent parameters of this simplified model are the gluino and lightest neutralino masses $m_{\tilde{g}}$ and $m_{\tilde{\chi}_1^0}$. The chargino and second-lightest neutralino masses are given in terms of these inputs by

$$m_{\tilde{\chi}_1^\pm} = \frac{1}{2}(m_{\tilde{g}} + m_{\tilde{\chi}_1^0}) \quad \text{and} \quad m_{\tilde{\chi}_2^0} = \frac{1}{2}(m_{\tilde{\chi}_1^\pm} + m_{\tilde{\chi}_1^0}). \tag{2}$$

[b] Despite the true number of steps in this decay, ATLAS refers to this as a "two-step" simplified model.

The mass of the off-shell squark mediating the initial three-body decay is not specified. The cut-flows provided by ATLAS apply to the mass point $(m_{\tilde{g}}, m_{\tilde{\chi}_1^0}) = (1600, 100)$ GeV. We validate our implementation by generating an event sample according to ATLAS' specifications and comparing the event yields for this sample in each signal region in MadAnalysis 5 to those reported by ATLAS.

3.1. *Event generation*

The popular matrix element generator MadGraph5_aMC@NLO (MG5_aMC) is shipped[23,24] with an implementation of the Minimal Supersymmetric Standard Model (MSSM)[25] compatible with the second SUSY Les Houches Accords (SLHA2) conventions for tabulating mass spectra and unstable particle decays.[26] In order to obtain an event sample suitable for comparison to ATLAS' benchmark results, we simulate the gluino pair-production process described above in the `MSSM_SLHA2` model[27] loaded by MG5_aMC version 3.1.0. For definiteness, we take $q = u$, $q' = d$, and $\tilde{q} = \tilde{u}_{\mathrm{L}}$.

We use MG5_aMC to generate 10^5 events with a hard-scattering amplitude computed at leading order (LO) in the strong coupling. The matrix element, which includes the gluino pair production with the emission of up to two additional partons, is convolved with the NNPDF 2.3 LO set of parton distribution functions.[28] The hard-scattering results are matched to parton showers with the aid of Pythia 8 version 8.244,[29] which also simulates hadronization and crucially handles the decays of the pair-produced gluinos[c]. Pythia is called with the A14 tune,[31] and the matching is performed according to the CKKW-L prescription[32] with a matching scale of $\mu_{\mathrm{match}} = m_{\tilde{g}}/4 = 400\,\mathrm{GeV}$. We then pass these showered and hadronized event samples to MadAnalysis 5 to initiate the analysis process described at the end of Section 2.2.

3.2. *Comparison with official results*

A comparison of our results and the official cut-flows for the three-step gluino decay model at the point $(m_{\tilde{g}}, m_{\tilde{\chi}_1^0}) = (1600, 100)$ GeV is available in Tables 4–11. These tables are collected in an appendix for easier reading. We provide one comparison table for each non-overlapping signal region in the analysis. In these tables, the efficiency ϵ_i of selection cut i is given by

$$\epsilon_i^X = \frac{N_i^X}{N_{i-1}^X},$$

where N_i^X is the number of events passing cut i in analysis $X \in \{\mathrm{ATLAS}, \mathrm{MA5}\}$, and $N_0^{\mathrm{MA5}} = N_0^{\mathrm{ATLAS}}$ are the total sample sizes set equal for direct comparison;

[c]Passing the gluino decays to Pythia, which results in the loss of spin correlations that could in principle be retained by including the cascade decays in the matrix element, is consistent with ATLAS' approach[30] and necessary in order to produce a sample with up to two additional partons in a finite period of time.

and the discrepancy between the ATLAS and MadAnalysis 5 at each stage of the selection strategy is given by

$$\delta_i = \frac{\epsilon_i^{\mathrm{MA5}}}{\epsilon_i^{\mathrm{ATLAS}}} - 1.$$

The agreement is good, ranging from negligible to around twenty percent depending on signal region, but generally hovering around the ten-percent level. The largest sources of error are jet-related selection cuts, with the standard-jet multiplicity cuts particularly performing more poorly with rising N_{jet}. On the other hand, the proxy cut on missing transverse energy significance $\mathcal{S}(E_{\mathrm{T}}^{\mathrm{miss}})$ performs better than expected, and the b-jet tagging performance is acceptable in the two relevant signal regions. The exotic cuts on cumulative fat-jet mass M_{J}^{Σ} also correspond well to ATLAS' results. Altogether, we consider the agreement good enough to claim validation.

4. Conclusions

We have presented the implementation in MadAnalysis 5 of ATLAS-SUSY-2018-17, a search for new phenomena in final states with large jet multiplicities and significant missing transverse energy. This analysis can be used to constrain models of new physics featuring multijet signatures, including *e.g.* supersymmetric models predicting $t\bar{t}t\bar{t}$ production with kinematic structure distinct from the analogous SM process. This note updates our validation of ATLAS-CONF-2020-002, the predecessor of this analysis.[1] We have validated our implementation by simulating the pair production of gluinos decaying by cascade to quarks, W and Z bosons, and lightest neutralinos $\tilde{\chi}_1^0$ — a simplified SUSY-inspired model considered by the ATLAS collaboration in its report — and comparing the event yields after selection cuts in MadAnalysis 5 to those reported by ATLAS. We find acceptable agreement between our results and the ATLAS cut-flows and consider our implementation to be validated. The Delphes (detector simulation) and MadAnalysis recasting cards are available on the MadAnalysis 5 Public Analysis Database (PAD).

Acknowledgments

This work was supported in part by the United States Department of Energy under grant DE-SC0011726. Many thanks are due to Benjamin Fuks, whose assistance in refining the event generation and detector simulation proved invaluable.

References

1. T. Murphy, Implementation of the ATLAS-CONF-2020-002 analysis in MadAnalysis 5, `https://doi.org/10.14428/DVN/OUHTPC` (2021).
2. ATLAS Collaboration, G. Aad *et al.*, *JHEP* **10**, 062 (2020).
3. ATLAS Collaboration, G. Aad *et al.*, *JHEP* **11**, 099 (2011).
4. ATLAS Collaboration, G. Aad *et al.*, *JHEP* **07**, 167 (2012).
5. ATLAS Collaboration, G. Aad *et al.*, *JHEP* **10**, 130 (2013).
6. ATLAS Collaboration, G. Aad *et al.*, *Phys. Lett. B* **757**, 334–355 (2016).
7. ATLAS Collaboration, M. Aaboud *et al.*, *JHEP* **12**, 034 (2017).
8. L. M. Carpenter, T. Murphy and M. J. Smylie, *JHEP* **11**, 024 (2020).
9. L. M. Carpenter, T. Murphy and M. J. Smylie, `arXiv:2107.13565` (2021).
10. E. Conte, B. Dumont, B. Fuks and C. Wymant, *Eur. Phys. J. C* **74**, 10 (2014).
11. E. Conte and B. Fuks, *Int. J. Mod. Phys. A* **33**, 28 (2018).
12. J. Y. Araz, M. Frank and B. Fuks, *Eur. Phys. J. C* **80**, 6 (2020).
13. ATLAS Collaboration, G. Aad *et al.*, *JHEP* **10**, 062 (2020).
14. M. Cacciari, G. P. Salam and G. Soyez, *JHEP* **04**, 063 (2008).
15. ATLAS Collaboration, *ATL-PHYS-PUB-2016-012*, tech. rep. (June 2016).
16. ATLAS Collaboration, G. Aad *et al.*, *Eur. Phys. J. C* **79**, 11 (2019).
17. ATLAS Collaboration, *ATLAS-CONF-2018-038*, tech. rep. (July 2018).
18. B. Dumont, B. Fuks, S. Kraml *et al.*, *Eur. Phys. J. C* **75**, 2 (2015).
19. ATLAS Collaboration, M. Aaboud *et al.*, *JHEP* **12**, 034 (2017).
20. J. de Favereau, C. Delaere, P. Demin, A. Giammanco, V. Lemaître, A. Mertens and M. Selvaggi, *JHEP* **02**, 057 (2014).
21. M. Cacciari, G. P. Salam and G. Soyez, *Eur. Phys. J. C* **72**, 3 (2012).
22. A. L. Read, *J. Phys. G* **28**, 2693–2704 (2002).
23. J. Alwall, R. Frederix, S. Frixione, V. Hirschi, F. Maltoni, O. Mattelaer, H.-S. Shao, T. Stelzer, P. Torrielli and M. Zaro, *JHEP* **07**, 079 (2014).
24. R. Frederix, S. Frixione, V. Hirschi, D. Pagani, H.-S. Shao and M. Zaro, *JHEP* **07**, 185 (2018).
25. C. Csáki, *Mod. Phys. Lett. A* **11**, 599–613 (1996).
26. B. Allanach *et al.*, *Comput. Phys. Commun.* **180**, 8–25 (2009).
27. C. Duhr and B. Fuks, *Comput. Phys. Commun.* **182**, 11 (2011).
28. R. D. Ball, V. Bertone, S. Carrazza *et al.*, *Nucl. Phys. B* **867**, 244 (2013).
29. T. Sjöstrand, S. Ask, J. R. Christiansen, R. Corke, N. Desai, P. Ilten, S. Mrenna, S. Prestel, C. O. Rasmussen and P. Z. Skands, *Comput. Phys. Commun.* **191**, 159–177 (2015).
30. B. Fuks and T. Murphy, private correspondence (October 2021).
31. ATLAS Collaboration Collaboration, *ATLAS Pythia 8 tunes to 7 TeV data*, Tech. Rep. ATL-PHYS-PUB-2014-021, CERN (Geneva, 2020).
32. L. Lönnblad, *JHEP* **05**, 046 (2002).

Appendix A. Cut-flow comparison tables

Here we collect the tables comparing our results, obtained in MadAnalysis 5, to those provided by the ATLAS collaboration. Each table is labeled with the relevant signal region. Recall from Section 3.2 that the efficiency ϵ_i and error δ_i between ATLAS and MadAnalysis 5 of selection cut i are given by

$$\epsilon_i^X = \frac{N_i^X}{N_{i-1}^X},\ X \in \{\text{ATLAS}, \text{MA5}\}, \quad \text{and} \quad \delta_i = \frac{\epsilon_i^{\text{MA5}}}{\epsilon_i^{\text{ATLAS}}} - 1.$$

`SR-8ij50-0ib-MJ500`

Selection criterion	N_{events}		Cut efficiency ϵ		Discrepancy δ [%]
	ATLAS	MA5	ATLAS	MA5	
Events generated	1244.48	1244.48	—		—
$N_{\text{jet}}^{50} \geq 4$ ($\lvert\eta\rvert < 2.0$)	1072.91	1235.00	0.862	0.992	+15.11
$N_{\text{leptons}} = 0$	671.47	841.42	0.626	0.681	+8.863
$N_{\text{jet}}^{50} \geq 8$	453.63	530.79	0.676	0.631	−6.624
$M_{\text{J}}^{\Sigma} \geq 500\,\text{GeV}$	335.45	417.29	0.739	0.786	+6.312
$\mathcal{S}(E_{\text{T}}^{\text{miss}}) > 5$	260.19	290.48	0.776	0.696	−10.25

`SR-9ij50-0ib-MJ340`

Selection criterion	N_{events}		Cut efficiency ϵ		Discrepancy δ [%]
	ATLAS	MA5	ATLAS	MA5	
Events generated	1244.48	1244.48	—		—
$N_{\text{jet}}^{50} \geq 4$ ($\lvert\eta\rvert < 2.0$)	1072.91	1235.00	0.862	0.992	+15.11
$N_{\text{leptons}} = 0$	671.47	841.42	0.626	0.681	+8.862
$N_{\text{jet}}^{50} \geq 9$	310.62	350.13	0.463	0.416	−10.05
$M_{\text{J}}^{\Sigma} \geq 340\,\text{GeV}$	296.02	339.33	0.953	0.969	+1.696
$\mathcal{S}(E_{\text{T}}^{\text{miss}}) > 5$	230.12	234.65	0.777	0.692	−11.05

SR-10ij50-0ib-MJ340

Selection criterion	N_{events}		Cut efficiency ϵ		Discrepancy δ [%]
	ATLAS	MA5	ATLAS	MA5	
Events generated	1244.48	1244.48	—		—
$N_{\text{jet}}^{50} \geq 4$ ($\lvert\eta\rvert < 2.0$)	1072.91	1235.00	0.862	0.992	+15.11
$N_{\text{leptons}} = 0$	671.47	841.42	0.626	0.681	+8.863
$N_{\text{jet}}^{50} \geq 10$	178.02	186.72	0.265	0.222	−16.30
$M_{\text{J}}^{\Sigma} \geq 340\,\text{GeV}$	172.69	183.16	0.970	0.981	+1.124
$\mathcal{S}(E_{\text{T}}^{\text{miss}}) > 5$	132.57	121.41	0.768	0.663	−13.66

SR-10ij50-0ib-MJ500

Selection criterion	N_{events}		Cut efficiency ϵ		Discrepancy δ [%]
	ATLAS	MA5	ATLAS	MA5	
Events generated	1244.48	1244.48	—		—
$N_{\text{jet}}^{50} \geq 4$ ($\lvert\eta\rvert < 2.0$)	1072.91	1235.00	0.862	0.992	+15.11
$N_{\text{leptons}} = 0$	671.47	841.42	0.626	0.681	+8.863
$N_{\text{jet}}^{50} \geq 10$	178.02	186.72	0.265	0.222	−16.30
$M_{\text{J}}^{\Sigma} \geq 500\,\text{GeV}$	150.24	162.36	0.844	0.870	+3.032
$\mathcal{S}(E_{\text{T}}^{\text{miss}}) > 5$	113.63	107.84	0.756	0.664	−12.18

SR-10ij50-1ib-MJ500

Selection criterion	N_{events}		Cut efficiency ϵ		Discrepancy δ [%]
	ATLAS	MA5	ATLAS	MA5	
Events generated	1244.48	1244.48	—		—
$N_{\text{jet}}^{50} \geq 4$ ($\lvert\eta\rvert < 2.0$)	1072.91	1235.00	0.862	0.992	+15.11
$N_{\text{leptons}} = 0$	671.47	841.42	0.626	0.681	+8.863
$N_{\text{jet}}^{50} \geq 10$	178.02	186.72	0.265	0.222	−16.30
$N_{b\text{-jet}} \geq 1$	95.88	99.94	0.539	0.535	−0.618
$M_{\text{J}}^{\Sigma} \geq 500\,\text{GeV}$	82.63	85.85	0.862	0.859	−0.323
$\mathcal{S}(E_{\text{T}}^{\text{miss}}) > 5$	61.56	55.83	0.745	0.650	−12.71

SR-11ij50

Selection criterion	N_{events}		Cut efficiency ϵ		Discrepancy δ [%]
	ATLAS	MA5	ATLAS	MA5	
Events generated	1244.48	1244.48	—		—
$N_{\text{jet}}^{50} \geq 4$ ($\lvert\eta\rvert < 2.0$)	1072.91	1235.00	0.862	0.992	+15.11
$N_{\text{leptons}} = 0$	671.47	841.42	0.626	0.681	+8.863
$N_{\text{jet}}^{50} \geq 11$	81.40	78.48	0.121	0.093	−23.06
$\mathcal{S}(E_{\text{T}}^{\text{miss}}) > 5$	61.29	51.09	0.753	0.651	−13.54

`SR-12ij50-2ib`

Selection criterion	N_{events}		Cut efficiency ϵ		Discrepancy δ [%]
	ATLAS	MA5	ATLAS	MA5	
Events generated	1244.48	1244.48	—		—
$N_{\text{jet}}^{50} \geq 4$ ($\lvert\eta\rvert < 2.0$)	1072.91	1235.00	0.862	0.992	+15.11
$N_{\text{leptons}} = 0$	671.47	841.42	0.626	0.681	+8.863
$N_{\text{jet}}^{50} \geq 12$	29.20	31.34	0.043	0.037	−14.35
$N_{b\text{-jet}} \geq 2$	7.58	10.14	0.260	0.324	+24.63
$\mathcal{S}(E_{\text{T}}^{\text{miss}}) > 5$	5.30	6.45	0.699	0.636	−8.988

`SR-9ij80`

Selection criterion	N_{events}		Cut efficiency ϵ		Discrepancy δ [%]
	ATLAS	MA5	ATLAS	MA5	
Events generated	1244.48	1244.48	—		—
$N_{\text{jet}}^{50} \geq 4$ ($\lvert\eta\rvert < 2.0$)	1072.91	1235.00	0.862	0.992	+15.11
$N_{\text{leptons}} = 0$	671.47	841.42	0.626	0.681	+8.863
$N_{\text{jet}}^{80} \geq 9$	129.53	144.32	0.193	0.172	−11.09
$\mathcal{S}(E_{\text{T}}^{\text{miss}}) > 5$	96.49	96.49	0.745	0.644	−13.53